RAINBOW FILTERING FOR TERRAIN CORRECTING AIRBORNE GRAVITY

by

David L. Campbell

U.S. Geological Survey
P.O. Box 25046, Denver Federal Center
Denver, Colorado 80225

Open File Report 83-385

1983

ABSTRACT

In 1933, H. Rainbow derived a digital filter that relates horizontal gravity gradient to slope of the causative body. The Rainbow filter helps point to techniques for making topographic corrections to airborne gravity data.

INTRODUCTION

In a remarkable report that anticipated modern techniques of digital data processing, H. Rainbow (1934) published digital filters relating torsion balance gravity measurements to slopes of two- and three-dimensional causative bodies. The method languished, probably because it required many regularly spaced measurements along a profile and so would have been operationally cumbersome at the time. With the recent advent of airborne gravity techniques (LaCoste and others, 1982), such profiles should become more and more common, so that it is time to give Rainbow filters a second look.

The fundamental equation of Rainbow filtering is

$$s = R*T, \tag{1}$$

where s is the slope along the profile direction of the side of the causative body, R is the Rainbow filter, T represents the horizontal gradient of the gravity field along the profile direction, and * represents digital convolution. For the ideal case of two-dimensional source bodies striking perpendicular to the profile direction, the Rainbow filter coefficients are given by

$$R_n' = \frac{H}{D}\left[(-1)^n e^{\pi \frac{H}{D}} - 1\right] \Big/ 2\pi^2 G\sigma\left[n^2 + \left(\frac{H}{D}\right)^2\right], \tag{2}$$

where H = average vertical depth of top of source body, D = horizontal interval between measurements, G = universal gravitation constant, and σ = density difference between source body and its surroundings. If we take H = D, so that the observed data is sampled at intervals equivalent to the depth of interest for investigating source bodies, equation (2) reduces to

$$R_n = \left[(-1)^n e^{\pi} - 1\right] \Big/ 2\pi^2 G\sigma\,(n^2+1). \tag{3}$$

Numerical values of the coefficients $G\sigma R_n$ were given by Rainbow, and are graphed in figure 1. The Rainbow filter is symmetric, may be truncated at order N with 2N+1 coefficients (R_{-N}, R_{-N+1}, ... R_{-1}, R_o, R_1, ... R_{N-1}, R_N), and converges as $1/N^2$. Note that the numerical value of the coefficients is independent of truncation order N.

Terrain-correcting airborne gravity data

Suppose an airborne gravity survey is flown at constant altitude along a profile perpendicular to topography that is approximately two-dimensional. Suppose a radar altimeter or similar device measures vertical distance to the ground below the aircraft, and that this distance and the gravity field are digitally recorded at intervals corresponding to the average ground clearance. At profile-point i, the slope of the terrain below, s_i, and the horizontal gravity gradient, T_i, may be determined by an appropriate differencing scheme. Note that measured gravity gradient T_i will be the superposition of components due to terrain $T_i(t)$ and components due to geology $T_i(g)$.

$$T_i = T_i(t) + T_i(g) \tag{4}$$

At this point we regard the Rainbow filter as relating topographic slope s_i to terrain gradients only, so that

$$\begin{aligned} s &= R * T(t) \\ &= R * (T - T(g)). \end{aligned} \tag{5}$$

In equation (5), quantities s, R, and T are known, but T(g) is unknown and of interest to us. Hence we write

$$T(g) = T - R^{-1} * s \tag{6}$$

In words, horizontal gravity gradients may be terrain corrected by subtracting from the observed gravity gradient the convolution product of topographic slope with the inverse Rainbow filter.

Numerical simulation

Numerical simulation of the above process was done using a topographic feature consisting of a 2-km-wide flat-topped two-dimensional butte with a 6:1 slope on one side and a 2:1 slope on the other side. The butte was 1 km high and the gravity survey was "flown" 0.5 km above its top. Its density was 2.67 g/cm^3.

The calculations were performed using a Hewlett-Packard[1] Model 85 desktop calculator with a Matrix ROM. Using this equipment, equation (5) was treated by solving the matrix system

----

[1]The use of trade names is for descriptive purposes only and does not imply endorsement by the U.S. Geological Survey.

$$(7) \qquad \begin{pmatrix} S_1 \\ S_2 \\ S_3 \\ \cdots \end{pmatrix} = \begin{pmatrix} R_0 & R_1 & 0 & 0 & \cdots & 0 \\ R_1 & R_0 & R_1 & 0 & \cdots & 0 \\ 0 & R_1 & R_0 & R_1 & \cdots & 0 \\ & & & & & \cdots \\ 0 & \cdots & & & \cdots & R_0 \end{pmatrix} \begin{pmatrix} T_1 \\ T_2 \\ T_3 \\ \cdots \end{pmatrix} \quad \text{for } N=1.$$

Under this scheme, the inverse Rainbow filter was not calculated explicitly. No doubt, other, much more efficient numerical procedures for solving (7) could be devised that exploit the symmetry and sparseness of the Toeplitz-type matrix R.

Figure 2 shows Rainbow filter approximations to horizontal gravity gradient for filters of orders 2 through 7. The approximation is somewhat better for even orders than for odd ones, and (at least for this example) is nowhere good, and does not improve markedly for N greater than 4. In all cases, the filter has trouble handling the steep 2:1 slope, predicting higher gradients there than would actually be observed using first-order point-to-point differencing. Similarly, the filter gives a poor approximation along portions of the profile along which vertical distance to topography H and sampling distance D are not of comparable magnitude.

Figure 3 shows the effect of varying depth to sampling distance ratio H/D and sampling distance D over the same topographic feature. Because parameter D sets the scale of the calculation, the feature appears smaller for higher values of D. At the same time, calculated gravity gradients change due to the relatively coarser differencing distance. Clearly the Rainbow filter is de-tuned by using H/D ratios other than 1 (fig. 3a). There is some indication that the best choice for H=D is a distance from the highest peaks and that to the bottoms of the deepest valleys (figs. 3b, c). Figures 3c,d show a drawback of the Rainbow filter; namely, that it depends only on the ratio H/D so that its predicted gradients are independent of observation datum H. Obviously, however, true gradients do depend critically on this parameter.

Figure 4 shows the Rainbow filter estimate of gravity gradients for a draped survey. Here the observed gradient is exaggerated over that seen by the level survey of figure 2, but, because H=D, the Rainbow estimates are the same. Apparently the Rainbow filter does a better job with draped than level data.

In figures 5 and 6, the single-butte test topography is replaced by a two-hill test case. Again the Rainbow filter better approximates draped gradients (fig. 6) than level ones (fig. 5). Here, the optimum filter order is closer to N=3 ($3\,{}^1\!/_2$ km window $\approx$ length of left hill) or to N=5 ($5\,{}^1\!/_2$ km window $\approx$ length of right hill). Clearly the filter order should be chosen so as to match dominant wavelengths in the topography.

As derived, the Rainbow filter relates horizontal gravity gradients to horizontal gradients in topography. Clearly it ought to be possible to integrate both sides of the equation so as to relate gravity to topography directly. The Rainbow coefficients should be uneffected by this process, though the constant of integration will have to be found that shifts the Rainbow estimates by the proper amount to match the observed gravity. Figure 7 shows an effort along these lines, in which the integration constant was determined empirically in each case so as to (approximately) minimize RMS error. Again, using H=D, the same Rainbow estimates result whether the survey is supposed level or draped, but they fit the draped gravity better.

SUMMARY

The tests reported here represent attempts to numerically verify a half-century-old mathematical development. They show that the Rainbow filtering technique holds promise for terrain-correcting airborne gravity data in an on-line mode. From these numerical experiments it appears that the Rainbow filter is best tuned when H=D, but that this choice removes a degree of freedom in the solution so that exactly the same Rainbow estimates result for data which is draped or level, or flown at different levels. There appears to be a better fit to draped than to level data. The optimum order (length) of the filter appears to depend on frequency content of the topography, but is very modest given present-day microprocessor capabilities. The Rainbow filter estimates quite well horizontal gravity gradients due to terrain, but it estimates total gravity due to terrain less well. (RMS errors are of the order of twice the 5-mGal precision of the present generation of airborne gravity measurements). This report considered two-dimensional topography only, but Rainbow gives the corresponding filter for the three-dimensional case in his paper. Similar filters for vertical gravity gradients, and for magnetic surveys, may be derived but will be different from the common horizontal gravity gradient-total gravity filter tested here. Shaping and optimization of such filters using modern filter design techniques definitely should be tried, given the degree of success attained using only the naive techniques reported here. Perhaps this study will encourage development and refinement of other techniques to filter topographic effects from airborne gravity and magnetic data.

References cited:

Rainbow, H., 1934, The interpretation of torsion balance data: Proceedings of the World Petroleum Congress, London, v. 1, pps. 143-6.

LaCoste, L., Ford, J., Bowles, R., and Archer, K., 1982, Gravity measurements in an airplane using state-of-the-art navigation and altimetry: Geophysics, v. 47, no. 5, pps. 832-838.

APPENDIX - Mathematical Development

Because Rainbow's report may not be available in many libraries today, the following repeats and expands upon his derivation of eqn. (1):

Start with the (vertical component of) gravity field due to a two-dimensional body, as observed at altitude H.

(A-1) $$g(x,H) = \int_\xi \int_\zeta \frac{2G\rho(\xi,\zeta)\,(H-\zeta)\,d\zeta\,d\xi}{(H-\zeta)^2 + (x-\xi)^2} \, .$$

This equation comes from integrating the two-dimensional Green's function $2z/(x^2+z^2)$ over the cross-section of the body. In other words

(A-2) $$\nabla^2 \left[z/(x^2+z^2) \right] = \pi\,\delta(x)\,\delta(z) \, .$$

Because Rainbow was working with torsion-balance instruments, he determined the horizontal gradient

(A-3) $$g_{,x}(x,H) = \int_\xi \int_\zeta \frac{-4G\rho(\xi,\zeta)(H-\zeta)(x-\xi)}{\left[(H-\zeta)^2 + (x-\xi)^2\right]^2}\,d\zeta\,d\xi .$$

Now approximate the effect of 2-D topography of height $h(\xi)$ by supposing it to be condensed onto the topographic datum $\zeta=0$. We write

(A-4) $$\rho(\xi,\zeta) = \rho\, h(\xi)\,\delta(\zeta) \, .$$

Substitution into (A-3) gives

(A-5) $$g_{,x}(x,H) = -2G\rho H \int_\xi \frac{2(x-\xi)}{\left[H^2+(x-\xi)^2\right]^2}\, h(\xi)\,d\xi .$$

Note that

(A-6) $$\frac{\partial}{\partial\xi}\left[\frac{1}{\left[H^2+(x-\xi)^2\right]}\right] = \frac{2(x-\xi)}{\left[H^2+(x-\xi)^2\right]^2} \, .$$

Integrating (A-5) by parts

(A-7) $$g_{,x}(x,H) = 2G\rho \int_{\xi} \frac{H}{H^2+(x-\xi)^2} \frac{\partial h(\xi)}{\partial \xi} d\xi .$$

This is Rainbow's equation, though derived differently. Equation (A-7) gives horizontal gravity gradient as a weighted integral of topographic gradient, and is of the filter form we desire. Thus (A-7) represents a promising starting point for future efforts. Rainbow, however, was concerned with the inverse problem, that of finding gradients of buried topography from observed horizontal gravity gradients. We continue his deviation.

Comparing with (A-2) gives

(A-8) $$2\pi G h_{,x}(x) = g_{,x}(x,o) .$$

The gravity gradient on topographic datum z=o is a constant times the topographic gradient.

Suppose $g_{,x}$ is known at 2M points in the interval (L, $L-\frac{L}{M}$), evenly spaced at interval D=L/M, so we may fit the Fourier Series

(A-9) $$g_{,x}(x,H) = \sum_{n=1}^{M} A_n \cos\frac{\pi n}{L}x + B_n \sin\frac{\pi n}{L}x .$$

where

(A-10) $$A_n = \frac{1}{M} \sum_{k=-M}^{M-1} g_{,x}(kD,H) \cos\frac{\pi n}{M}k .$$

In the limit as $M \rightarrow \infty$

(A-11) $$g_{,x}(x,H) \rightarrow \int_0^1 \left[A(\lambda)\cos\frac{\pi\lambda x}{D} + B(\lambda)\sin\frac{\pi\lambda x}{D}\right] d\lambda ,$$

where

(A-12) $$A(\lambda) = \sum_{k=-\infty}^{\infty} g_{,x}(kD,H) \cos\pi k\lambda .$$

Because $g_{,x}$ is harmonic, we may downward continue from level H to topographic datum z=o:

(A-13)
$$g_{,x}(x,0)=\int_0^1 e^{\pi\lambda\frac{H}{D}}\left[A(\lambda)\cos\frac{\pi\lambda x}{D}+B(\lambda)\sin\frac{\pi\lambda x}{D}\right]d\lambda.$$

But

(A-14)
$$\begin{aligned}g_{,x}(0,0)&=\int_0^1 e^{\pi\lambda\frac{H}{D}}A(\lambda)\,d\lambda\\&=\int_0^1 e^{\pi\lambda\frac{H}{D}}\sum_{k=-\infty}^{\infty}g_{,x}(kD,H)\cos\pi k\lambda\,d\lambda\\&=\sum_{k=-\infty}^{\infty}g_{,x}(kD,H)\int_0^1 e^{\pi\lambda\frac{H}{D}}\cos\pi k\lambda\,d\lambda\\&=\sum_{k=-\infty}^{\infty}g_{,x}(kD,H)\frac{H}{D}\left[(-1)^k e^{\pi\frac{H}{D}}-1\right]\Big/\pi\left[k^2+\left(\frac{H}{D}\right)^2\right].\end{aligned}$$

Combining with (A-9) gives

(A-15)
$$h_{,x}(x)=\sum_{k=-\infty}^{\infty}g_{,x}(kD,H)\,\frac{\frac{H}{D}\left[(-1)^k e^{\pi\frac{H}{D}}-1\right]}{2\pi^2 G\rho\left[k^2+\left(\frac{H}{D}\right)^2\right]}.$$

This is the result cited in equations (1) and (2).

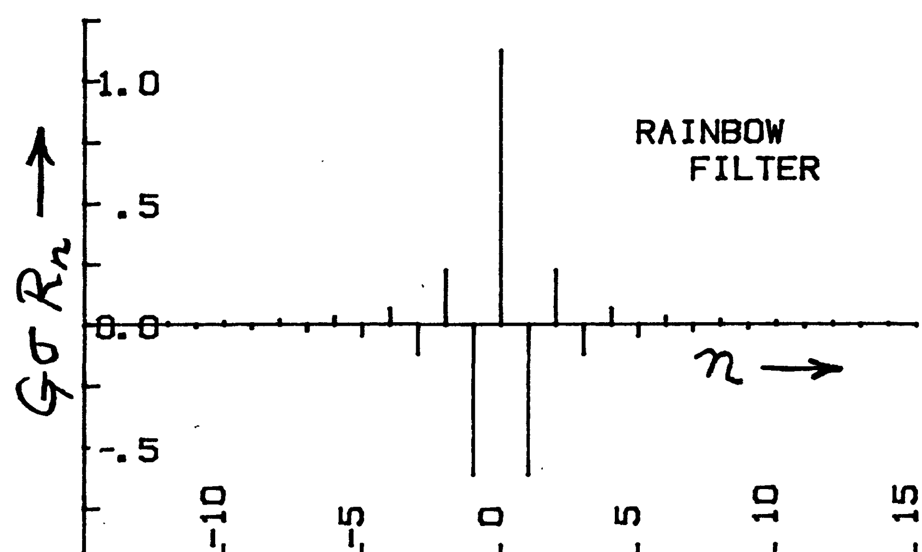

Fig. 1.--Chart showing normalized two-dimensional Rainbow filter.

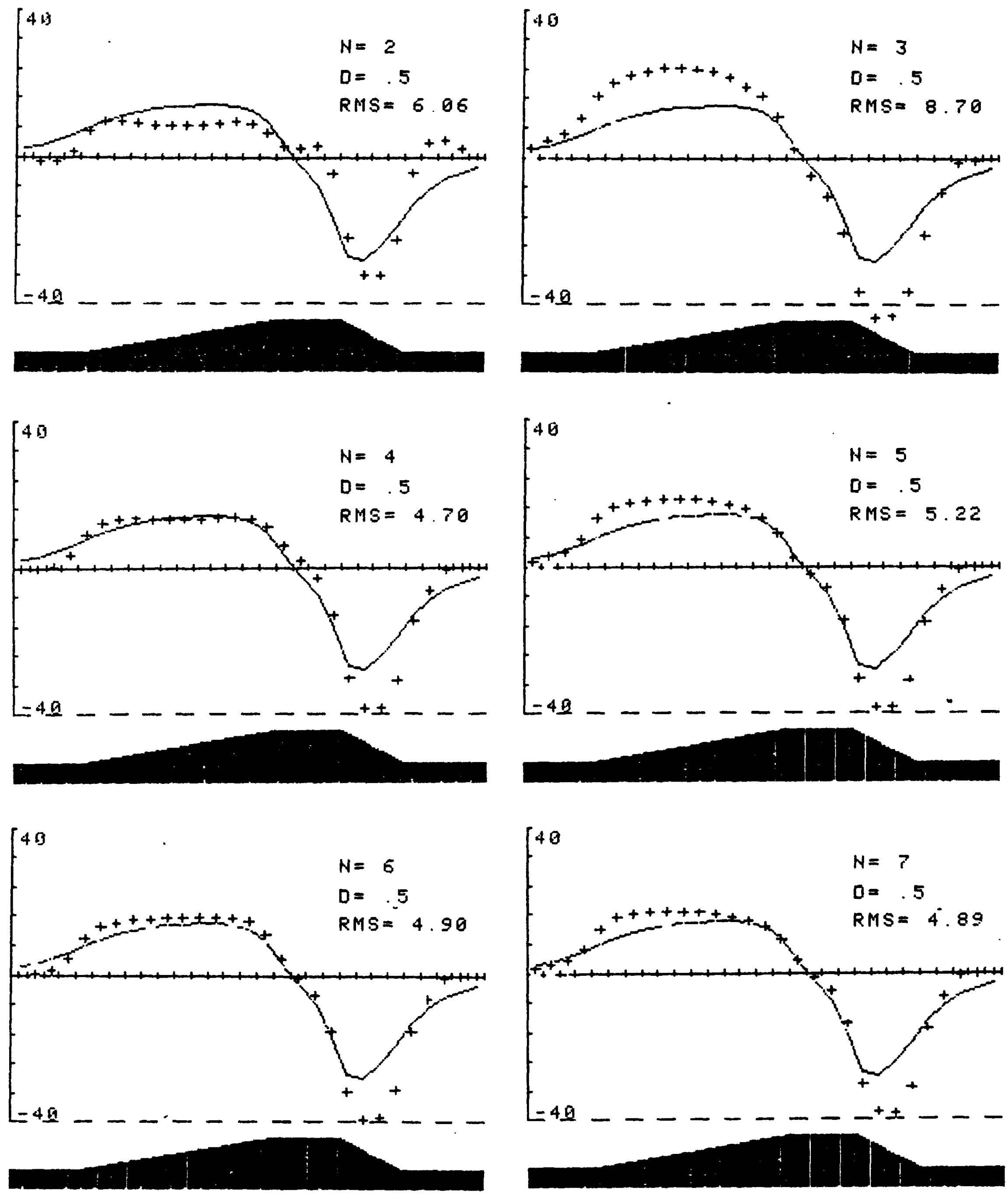

Fig. 2.--Rainbow filter estimates (+) of first order difference horizontal gravity gradient (------) as a function of filter order N. Topographic feature is a 2-D butte, (solid shading) 1 km high and 2 km wide at its top, having 6:1 and 2:1 side slopes. Gravity is sampled at 0.5 km intervals on a level observation datum (- - -) that passes 0.5 km over butte top. Units of profile curves are mGal/km. RMS represents root-mean-squared measure of error of fit between Rainbow estimates and gravity gradient, in mGal/km.

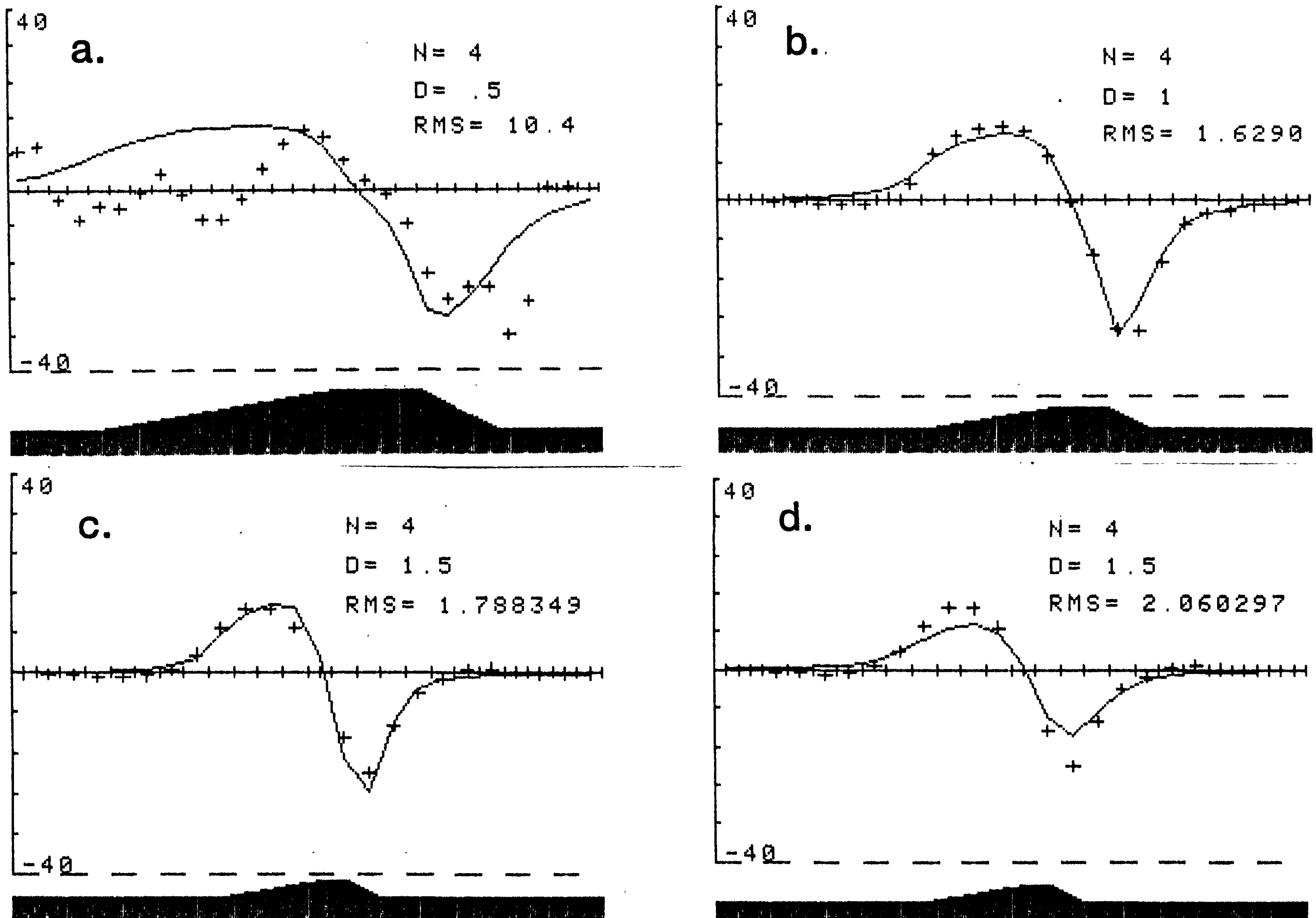

Fig. 3.--Effects of changing parameters H(=distance from observation datum to surface topography) and D(=observation interval). a. Ratio H/D allowed to vary by using average H at each plotting point in eqn. (2). D=0.5 km. Plotting points are midway between observation points. b. H=D=1 km= distance from observation datum (- - -) halfway down butte slope. Slightly better fits (not shown) are found for this case when N=6 (RMS=1.6116 mGal/km) and N=7 (RMS= 1.3239 mGal/km). c. H=D=1.5 km = distance from observation datum to plain at foot of butte. Best RMS fit is shown. d. Observation datum raised to 2.5 km. H=D=1.5 km = distance from observation datum to butte top.

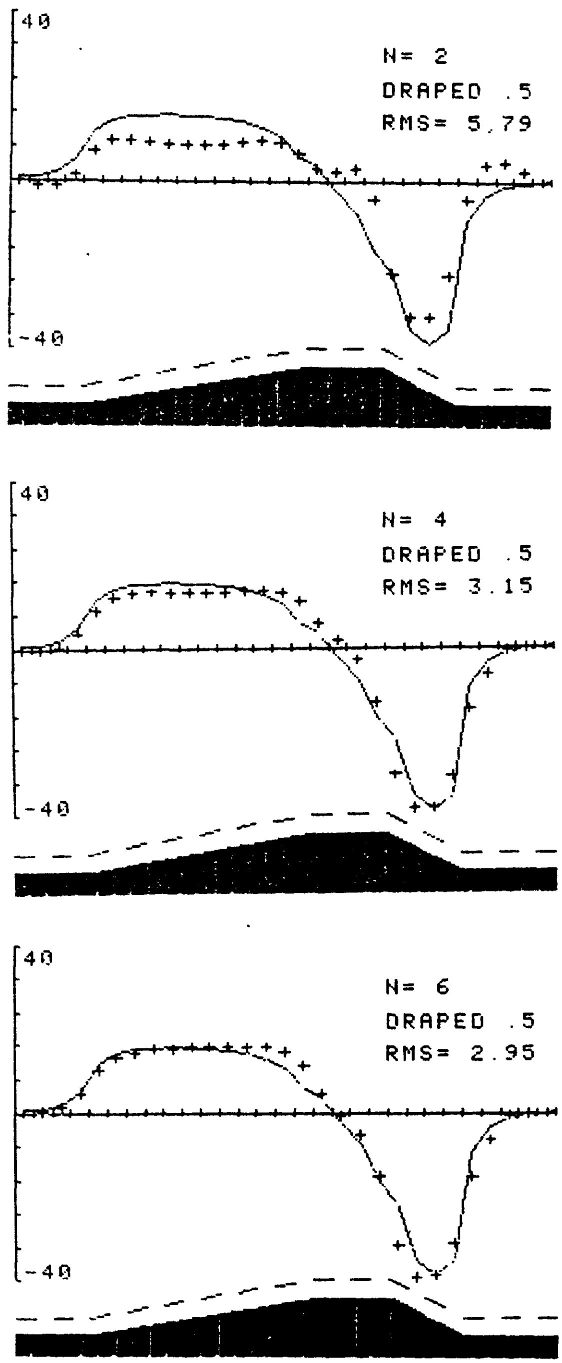

Fig. 4.--Gravity gradients observed on an observation datum draped at D=0.5 km above topography. For each order N, Rainbow filter estimates are the same as those for Fig. 2, but the match to the draped gradients is better.

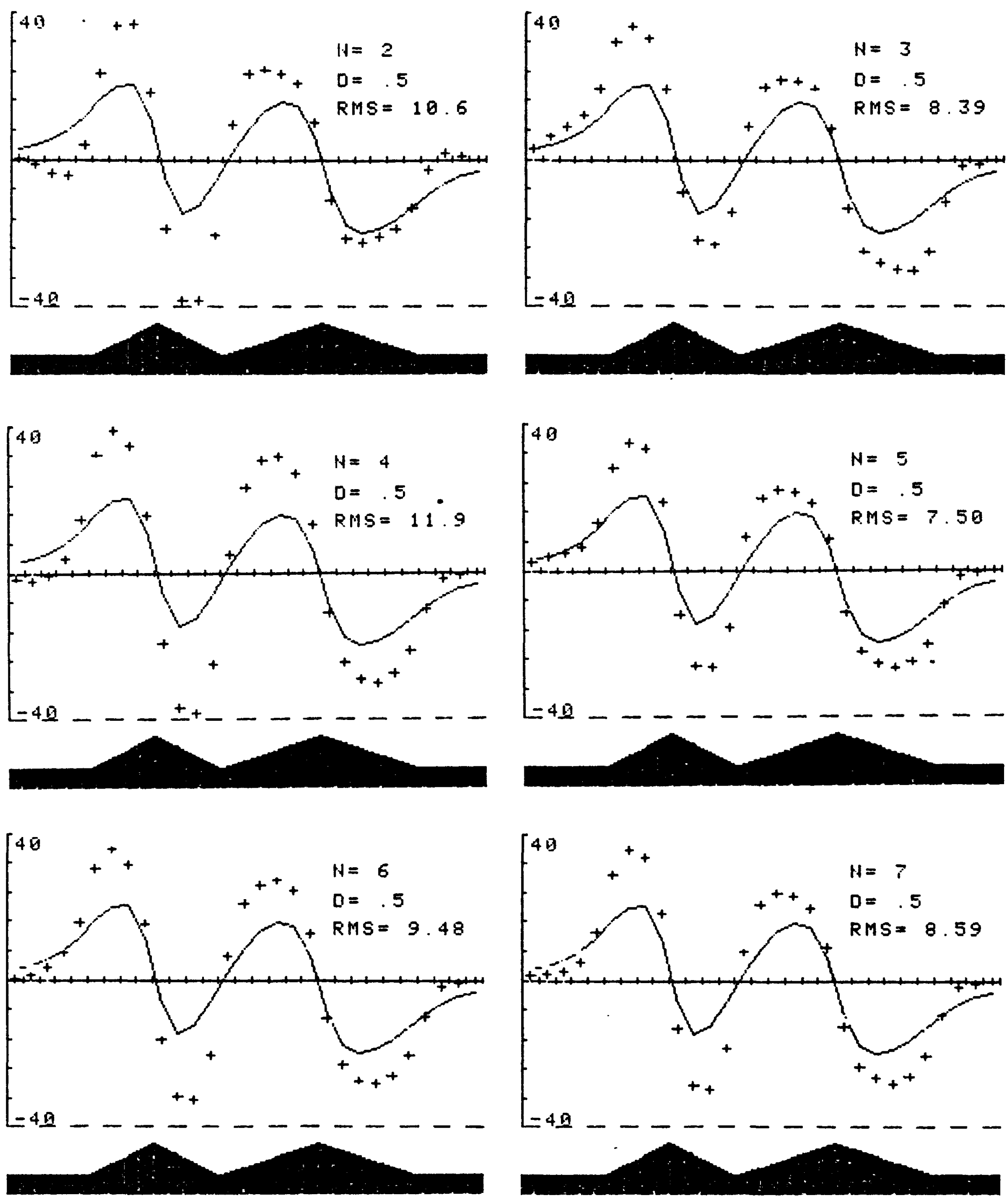

Fig. 5.--Rainbow filter estimates for various orders N of gravity gradients on a level observation datum for a two-hill model.

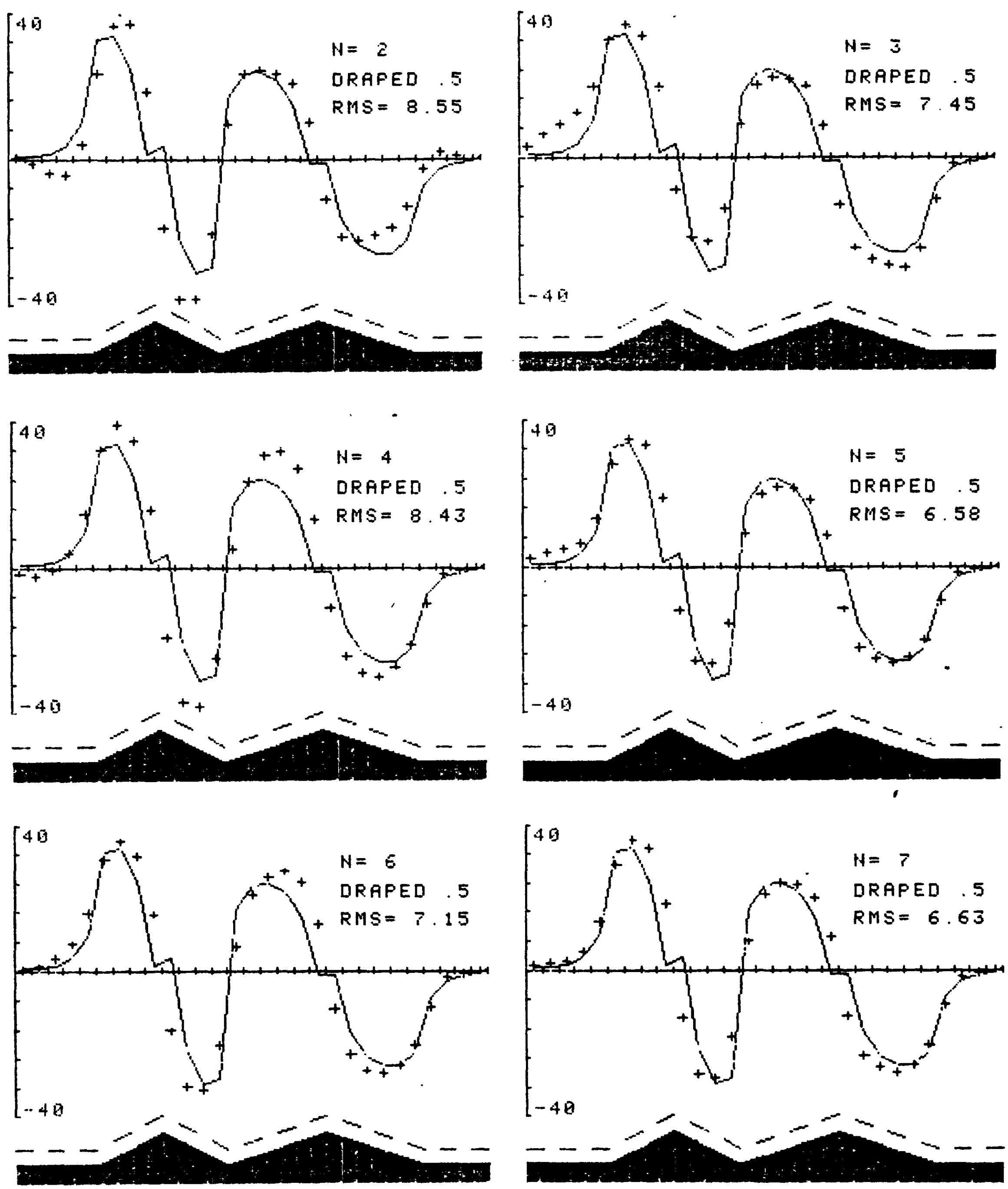

Fig. 6.--Rainbow filter estimates for various orders N of gravity gradients on a draped observation datum, for a two-hill model.

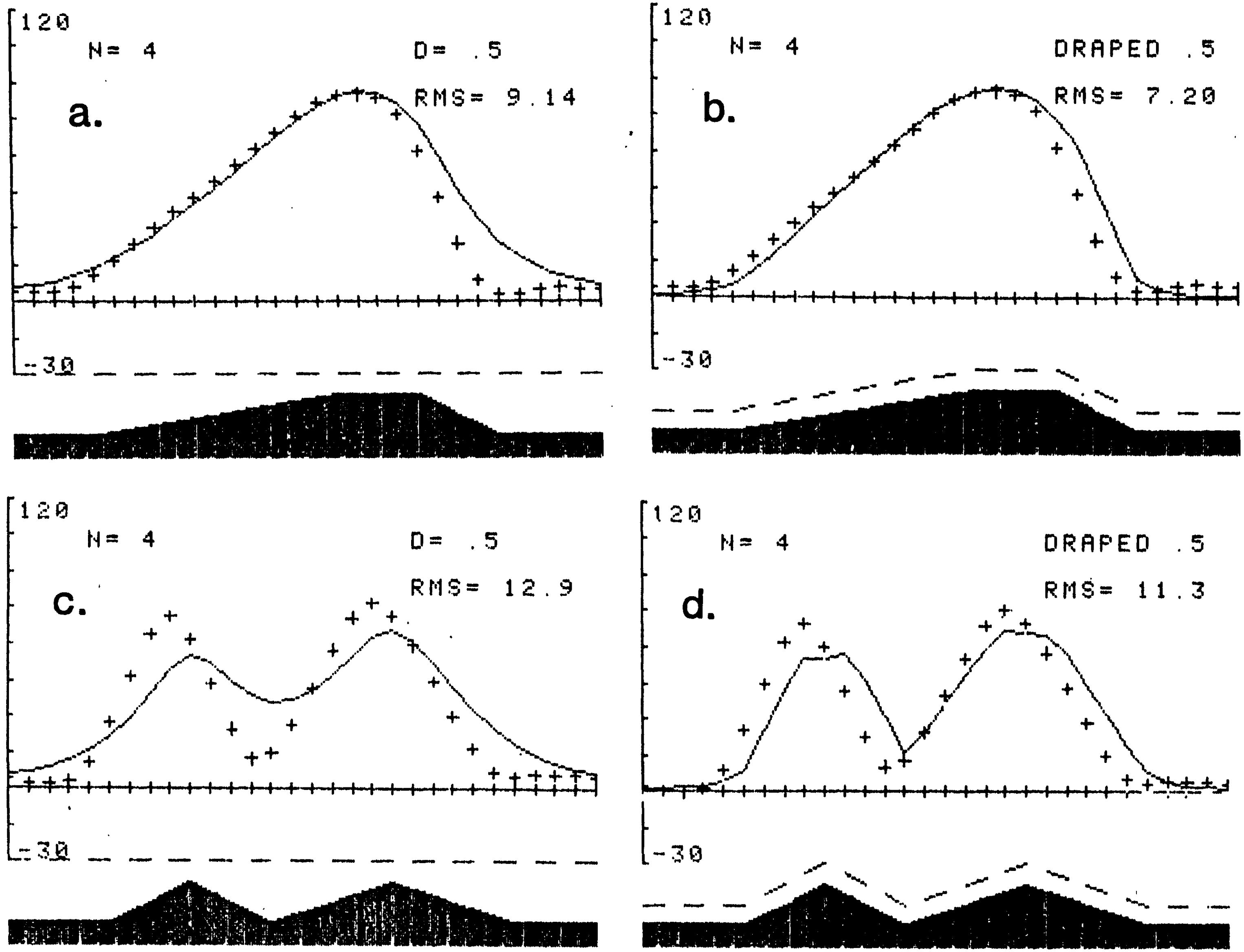

Fig. 7.--Rainbow filter estimates for order N=4 of total gravity (mGal). a. Level observation datum, single butte model. b. Draped observation datum, single butte model. c. Level observation datum, two-hill model. d. Draped observation datum, two-hill model.